IEEE Access
Multidisciplinary : Rapid Review : Open Access Journal

Received 26 November 2022, accepted 17 December 2022, date of publication 26 December 2022, date of current version 2 January 2023.

Digital Object Identifier 10.1109/ACCESS.2022.3232464

RESEARCH ARTICLE

H_∞ Loop Shaping Using Polytopic Weights and Pole Assignment to Missile Autopilot

YURI M. TAVARES[1] **AND JACQUES WALDMANN**[2]

[1]Weapon Systems Directorate, Marinha do Brasil, Rio de Janeiro 20010-000, Brazil
[2]Systems and Control Department, Instituto Tecnológico de Aeronáutica, São José dos Campos, São Paulo 12228-900, Brazil

Corresponding author: Yuri M. Tavares (yurimtavares@yahoo.com.br)

ABSTRACT Modern missiles must deal with stringent performance requirements and ensure robustness across a wide range of operating conditions during flight time. Classic gain-scheduling designs have been successful in practice, but do not provide theoretically ensured bounds on both performance and robustness. Controllers are interpolated at intermediate operating conditions and switching them may cause instability. On the other hand, polytopic linear parameter-varying (LPV) controllers avert this switching and use real-time information about the plant, in order to smooth out the gain scheduling. We hereby propose a novel procedure to yield an output feedback LPV controller that ensures robust H_∞ performance to a missile longitudinal autopilot. Our novel approach considers the four-block loop-shaping H_∞ control theory with polytopic LPV weights that use polytopic coordinates of the LPV plant. One is capable of adjusting the singular values of the open-loop plant individually at the polytope vertices, and benefits from a trade-off between linear matrix inequalities (LMI) based optimization tools and the designer experience. This can be construed as a natural extension of the traditional H_∞ loop-shaping method that uses linear time-invariant (LTI) weights. Assuming the scheduling variables are frozen, we also include LMI conditions for assigning closed-loop poles and hence circumvent controller order reduction. Nonlinear simulations assess the proposed autopilot, and results show an improved robust stability margin, in addition to an improved response to the acceleration command, concerning the LTI-based approach.

INDEX TERMS Autopilot, loop shaping, missile, pole assignment, polytopic, robust LPV.

I. INTRODUCTION

Missile autopilot design is a challenging task, because it must meet strict performance requirements, while ensuring robustness across a wide range of operating conditions [1]. The H_∞ loop-shaping theory [2] offers a good solution for this multi-objective purpose. Aeronautical applications include robust autopilots for flexible missiles [3], static controllers for manned [4] and unmanned helicopters [5], robust autopilots for agile missiles [6], 6-degree-of-freedom controllers for quadcopters with tilting rotor [7], and robust controllers for vertical takeoff-and-landing drones [8]. Using LMI optimization techniques [9], the sub-optimal controllers ensure performance, robustness, control action minimization, and noise attenuation.

The associate editor coordinating the review of this manuscript and approving it for publication was Mou Chen.

Under a classic gain scheduling scenario, LTI controllers are designed at selected operating points and interpolated at intermediate conditions of the flight envelope [1]. Whereas working well in practice, robustness and performance are not theoretically ensured [10]. Controllers switching may cause instability in fast varying systems. LPV controllers avert switching and provide smooth gain scheduling using measured variables during flight. Different lines of approach are based on polytopic representation, linear fractional transformation (LFT) representation, and linearization on a gridded domain. Important results extending H_∞ loop shaping to polytopic LPV systems arise in the design of an autopilot for a bank-to-turn missile [1], static output feedback control to missile [11] and unmanned aircraft [12], gain-scheduling control for a hovering vehicle [13], discrete-time static control for a vertical takeoff-and-landing aircraft [14], and controller design for a variable stiffness actuator [15].

In LFT representation, the LPV issue is construed as a robust performance problem for the nominal LTI plant along with LFT uncertainty. The uncertainty is a time-varying matrix-valued parameter that evolves in a convex polytope [16]. Previously, the translation and scaling of the scheduling variables were used to describe plant uncertainty in LFT form, and to generate an LPV model in addition to the H_2/H_∞ LPV controller for a missile longitudinal autopilot [17]. Differently, we use here the H_∞ loop shaping, taking into account the time-varying plant as an LPV model, whose state-space matrices evolve in convex polytopes. Moreover, a normalized coprime factor stabilization provides robustness to the closed-loop system. Weights are selected to ensure the open-loop properties at both high and low frequencies, and also to maximize the robust stability margin.

Previous work was grounded on a grid-based mixed sensitivity H_∞ approach to find an LPV controller for improving wheelset stability of railway vehicles [18], and for a small helicopter [19]. The latter linearizes the nonlinear plant model in a grid, which is composed of several operating conditions of the helicopter dynamics, and uses a common Lyapunov function to ensure robustness and performance to the entire flight envelope. The drawback is that the syntheses are only valid if the dynamics is linear between two design points. Also, the number of controllers increase with the number of design points.

The aforementioned H_∞ control references, except [12], handle LTI parameter-independent weights. Reference [12] uses weights that are directly dependent on the LPV plant scheduling variables. The setback is that the weights are specific for each problem. In the event the problem changes, the shaped plant must be redesigned. Reference [15] uses LTI weights and the plant is shaped equally in all polytope vertices. This is traditional in H_∞ loop-shaping LPV control solutions, and the design is less flexible. Missiles have a wide range of operating conditions along the interception path that depend on angle of attack, airspeed and altitude. Our main motivation contributing is to develop a more flexible and less conservative synthesis process to yield H_∞ loop-shaping LPV controllers for this kind of parameter-dependent plants.

We propose the use of weights that are not only parameter-dependent, but are also polytopic. The polytopic weights are capable of assuming any transfer functions, and are related to the LPV plant concerning their polytopic coordinates. One adjusts the singular values of the open-loop plant individually at the polytope vertices and can benefit from a trade-off between LMI-based automated design tools, in addition to the designer experience. We also use LMI conditions for assigning closed-loop poles, for the frozen values of the scheduling variables, in the desired frequency range. It prevents the fast dynamics usually present in high-order controllers synthesized with LMI optimization tools. Although model reduction techniques could be useful (see e.g., [17]), the full-order controller is desirable to ensure performance and robustness. Nonlinear simulations assess the proposed polytopic LPV control applied to a missile longitudinal autopilot. Since just a few output measurements are available in flight, our focus is on the output feedback.

We organized the paper as follows. Section II reviews theoretical concepts and also states the main problem. Section III details the missile polytopic LPV model. LMI conditions and the proposed methodology are presented in Section IV. Section V registers the autopilot design and its results. Finally, Section VI brings out the conclusions.

II. PRELIMINARIES

The notation is standard. $\mathbb{R}^{m\times n}$ is the set of $m \times n$ real matrices, $\mathbb{R}^n$ is the set of n-dimensional real vectors, whereas $\mathbb{C}$ is the set of complex numbers. For matrices or vectors Γ, Γ^T indicates transpose. $A > 0$ ($A < 0$) means that matrix A is a positive (negative) definite. I is the identity matrix containing appropriate dimensions, and I_n is the identity matrix $\in \mathbb{R}^{n\times n}$. The symbol $\bullet$ indicates a symmetric block in the matrices. $G = \left[\begin{array}{c|c} A & B \\ \hline C & D \end{array}\right]$ represents a state-space realization of a continuous-time system whose transfer function is $G(s) = C(sI - A)^{-1}B + D$. The symbol $\triangleq$ means "is defined as".

Definition 1 ([20]): Vertex representation.

$Co\{\Gamma_i\}_r$ is the convex hull of a finite number of vertices $\Gamma_1, \Gamma_2, \ldots, \Gamma_r$ with the same dimensions such that

$$Co\{\Gamma_i\}_r \triangleq \left\{\sum_{i=1}^{r} \upsilon_i\Gamma_i : \upsilon \in \Lambda\right\} \tag{1}$$

$$\upsilon \triangleq \left[\upsilon_1 \ \upsilon_2 \ \ldots \ \upsilon_r\right]^T \in \mathbb{R}^r \tag{2}$$

$$\Lambda \triangleq \left\{\lambda \in \mathbb{R}^r : \lambda_i \geq 0, \ \sum_{i=1}^{r} \lambda_i = 1\right\}. \tag{3}$$

Definition 2 ([20]): Polytopic LPV system.

An LPV system is called polytopic when state-space matrices are affine-dependent on a time-varying parameter vector $\theta(t)$ that takes values in a convex polytope $\Theta \triangleq Co\,\{\xi_i\}_r$.

Let us take into consideration a polytopic LPV system such that $\theta(t) \in \mathbb{R}^p$ with $r = 2^p$. Then, $\xi_i \in \mathbb{R}^p$ are the polytope vertices that bound $\theta(t)$, and the state-space matrices also belong to a convex polytope whose vertices are images of the ξ_i

$$\left[\begin{array}{c|c} A(\theta(t)) & B(\theta(t)) \\ \hline C(\theta(t)) & D(\theta(t)) \end{array}\right] \in Co\left\{\left[\begin{array}{c|c} A_i & B_i \\ \hline C_i & D_i \end{array}\right]\right\}_r \tag{4}$$

$$\left[\begin{array}{c|c} A_i & B_i \\ \hline C_i & D_i \end{array}\right] \triangleq \left[\begin{array}{c|c} A(\xi_i) & B(\xi_i) \\ \hline C(\xi_i) & D(\xi_i) \end{array}\right] \tag{5}$$

where $A(\theta(t)) \in \mathbb{R}^{n\times n}$, $B(\theta(t)) \in \mathbb{R}^{n\times n_u}$, $C(\theta(t)) \in \mathbb{R}^{n_y\times n}$, and $D(\theta(t)) \in \mathbb{R}^{n_y\times n_u}$. From the vertex representation, we rewrite $\theta(t)$ and the state-space matrices, using the same polytopic coordinates $a_i(t)$

$$\theta(t) = \sum_{i=1}^{r} a_i(t)\xi_i, \ a_i(t) \geq 0, \ \sum_{i=1}^{r} a_i(t) = 1 \tag{6}$$

$$\left[\begin{array}{c|c} A(\theta(t)) & B(\theta(t)) \\ \hline C(\theta(t)) & D(\theta(t)) \end{array}\right] = \sum_{i=1}^{r} a_i(t)\left[\begin{array}{c|c} A_i & B_i \\ \hline C_i & D_i \end{array}\right] \tag{7}$$

$$a(t) \triangleq \left[a_1(t)\ a_2(t)\ \ldots\ a_r(t)\right]^T \tag{8}$$

where $a_i(t) \in \mathbb{R}$, and $a(t) \in \mathbb{R}^r$ also belongs to the unit simplex Λ for each instant t.

Definition 3: Quadratic H_∞ performance.

Given $\gamma > 0$, a polytopic LPV system has the quadratic H_∞ performance $J_\infty(.) < \gamma$ if and only if it is asymptotically stable and the L_2-gain of the input-to-output map is lower than γ along all possible parameter trajectories $\theta(t)$ in the polytope Θ.

Lemma 1 ([20]): Bounded Real Lemma with quadratic H_∞ performance.

Consider $\gamma > 0$, a polytopic LPV system such as (7) is asymptotically stable with $J_\infty(.) < \gamma$ if and only if there is a symmetric positive definite matrix $X \in \mathbb{R}^{n\times n}$ to satisfy the set of LMI for $i = 1, \ \ldots\ , r$

$$\begin{bmatrix} A_i^T X + XA_i & XB_i & C_i^T \\ B_i^T X & -\gamma I & D_i^T \\ C_i & D_i & -\gamma I \end{bmatrix} < 0. \tag{9}$$

Remark 1: When $\theta(t)$ is a frozen p-dimensional vector, an LPV system reduces to an LTI system, (9) is known as the Bounded Real Lemma and $J_\infty(.)$ is the H_∞-norm $\|.\|_\infty$.

Lemma 2 ([21]): Closed-loop pole assignment constraints.

Consider the vertical strip defined in the complex plane as

$$\Upsilon \triangleq \{d + je \in \mathbb{C} \ :\ -d_1 < d < -d_2 \leq 0\} \tag{10}$$

where $d_1 > 0$ and $d_2 \geq 0$. From [21, theorem 2.2 and corollary 2.3], a matrix A has all its eigenvalues in Υ if and only if there is a symmetric positive definite matrix X with compatible dimensions such that

$$A^T X + XA + 2d_1 X > 0 \tag{11}$$
$$A^T X + XA + 2d_2 X < 0. \tag{12}$$

The H_∞ loop shaping was originally proposed for LTI systems by [2] and is comprised by two main stages:

1) using a pre-compensator $W_1(s)$ and a post-compensator $W_2(s)$, the open-loop frequency response of the plant $G(s)$ is shaped with the purpose to yield the desired singular values, where $G_s(s) = W_2(s)G(s)W_1(s)$; and
2) the shaped plant $G_s(s)$ is robustly stabilized by $K(s)$. The final feedback controller to the plant $G(s)$ is $K_F(s) = W_1(s)K(s)W_2(s)$.

Since the pair $\tilde{M}(s)$ and $\tilde{N}(s)$ is a normalized left coprime factorization for the shaped plant, we have

$$G_s(s) = \tilde{M}^{-1}(s)\tilde{N}(s) \tag{13}$$

and the perturbed system is

$$G_s(s) = (\tilde{M}(s) + \Delta_{\tilde{M}})^{-1}(\tilde{N}(s) + \Delta_{\tilde{N}}) \tag{14}$$

where $\Delta_{\tilde{M}}$ and $\Delta_{\tilde{N}}$ are coprime factorization uncertainties. Controller $K(s)$ solves the normalized left coprime factor robust stabilization problem if and only if it solves the following four-block H_∞ control problem [22, lemma 18.4 and corollary 18.5]:

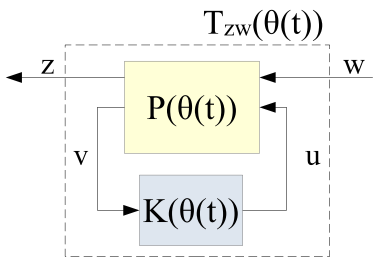

FIGURE 1. Diagram for the output feedback H_∞ control problem for polytopic LPV systems.

$$\|T_{zw}(s)\|_\infty = \left\| \begin{bmatrix} K(s) \\ I \end{bmatrix} H(s) \begin{bmatrix} I & G_s(s) \end{bmatrix} \right\|_\infty < \frac{1}{\epsilon_0} = \gamma \tag{15}$$

where $T_{zw}(s)$ is the closed-loop transfer function, $H(s) = (I + G_s(s)K(s))^{-1}$, and ϵ_0 is the robust stability margin. Using the small gain theorem [22, theorem 9.1], the controller design is robust to small disturbances embedded in the normalized left coprime factorization if and only if

$$\left\| \begin{bmatrix} \Delta_{\tilde{N}} & \Delta_{\tilde{M}} \end{bmatrix} \right\|_\infty \leq \epsilon_0. \tag{16}$$

We use this theorem to take into account wind, angle of attack estimation error, and other disturbance sources in the robust autopilot design.

Now, consider the main problem illustrated in Fig. 1. Given the shaped plant $G_s(\theta(t))$ in the form of (7) with $D(\theta(t)) = 0$, and its generalized plant $P(\theta(t))$ in the four-block loop shaping framework [12]

$$\begin{bmatrix} \dot{x} \\ z \\ v \end{bmatrix} = \overbrace{\sum_{i=1}^{r} a_i(t) \left[\begin{array}{c|cc} A_i & B_{1i} & B_{2i} \\ \hline C_{1i} & D_{11} & D_{12} \\ C_{2i} & D_{21} & 0 \end{array}\right]}^{P(\theta(t))} \begin{bmatrix} x \\ w \\ u \end{bmatrix} \leftrightarrow$$
$$\begin{bmatrix} \dot{x} \\ z_1 \\ z_2 \\ v \end{bmatrix} = \sum_{i=1}^{r} a_i(t) \left[\begin{array}{c|cc} A_i & \begin{pmatrix} 0 & B_i \end{pmatrix} & B_i \\ \hline \begin{pmatrix} 0 \\ C_i \end{pmatrix} & \begin{pmatrix} 0 & 0 \\ I & 0 \end{pmatrix} & \begin{pmatrix} I \\ 0 \end{pmatrix} \\ C_i & \begin{pmatrix} I & 0 \end{pmatrix} & 0 \end{array}\right] \begin{bmatrix} x \\ w_1 \\ w_2 \\ u \end{bmatrix} \tag{17}$$

that maps exogenous inputs $w \triangleq \left[w_1\ w_2\right]^T \in \mathbb{R}^{n_w}$ and control inputs $u \in \mathbb{R}^{n_u}$ to the controlled outputs $z \triangleq \left[z_1\ z_2\right]^T \in \mathbb{R}^{n_z}$, and measured outputs $v \in \mathbb{R}^{n_v}$, find a controller

$$K(\theta(t)) \triangleq \sum_{i=1}^{r} a_i(t) \left[\begin{array}{c|c} A_{ki} & B_k \\ \hline C_k & 0 \end{array}\right] \tag{18}$$

containing matrices $A_{ki} \in \mathbb{R}^{k\times k}$, $B_k \in \mathbb{R}^{k\times n_v}$, and $C_k \in \mathbb{R}^{n_u\times k}$ so that the output feedback law is $u(t) = K(\theta(t))v(t)$, and the closed-loop transfer function from w to z

$$T_{zw}(\theta(t)) \triangleq \sum_{i=1}^{r} a_i(t) \left[\begin{array}{c|c} A_{cl,i} & B_{cl,i} \\ \hline C_{cl,i} & D_{cl} \end{array}\right]$$

$$= \sum_{i=1}^{r} a_i(t) \left[\begin{array}{cc|c} A_i & B_{2i}C_k & B_{1i} \\ B_kC_{2i} & A_{ki} & B_kD_{21} \\ \hline C_{1i} & D_{12}C_k & D_{11} \end{array}\right] \quad (19)$$

satisfies quadratic H$_\infty$ performance $0 < J_\infty(T_{zw}(\theta(t))) < \gamma$ for all $\theta(t) \in \Theta$.

III. MISSILE POLYTOPIC LPV MODEL DERIVATION

From now, explicit time dependence of variables is omitted to ease the notation. Aerodynamic coefficients and their derivatives of the missile aerodynamics model are nonlinear functions of angle of attack α between -20^o and 20^o and Mach number M between 2 and 4. We now focus on the approaching end game, as the missile pursues the target using its onboard seeker, and the rocket motor has been completely burnt. The plant is nonminimum phase due to the actuators being at the rear of the missile. From the rigid-body dynamics equations, the missile nonlinear longitudinal model is

$$\dot{\alpha} = q + \frac{S_mQ_{din}cos(\alpha)\cdot\left(C_{z0} + \frac{C_{zq}qd_m}{2V_sM} + C_{z\delta}\delta_p\right)}{mV_sM} \quad (20)$$

$$\dot{q} = \frac{S_md_mQ_{din}\cdot\left(C_{m0} + \frac{C_{mq}qd_m}{2V_sM} + C_{m\delta}\delta_p\right)}{I_y} \quad (21)$$

$$a_{mz} = \frac{S_mQ_{din}\cdot\left(C_{z0} + \frac{C_{zq}qd_m}{2V_sM} + C_{z\delta}\delta_p\right)}{m} \quad (22)$$

where:

- α is the angle of attack (rad);
- q is the pitch rate (rad);
- δ_p is the pitch actuator (rad);
- a_{mz} is the missile acceleration in the body-z axis (m/s^2);
- $Q_{din} = 0.5\rho V_s^2M^2$ is the dynamic pressure (N/m^2);
- ρ is the air density (kg·m^3);
- V_s is the speed of sound (m/s);
- M is the Mach number;
- $S_m = 0.0216$ is the missile reference area (m^2);
- $d_m = 0.1660$ is the missile reference length (m);
- $m = 56.3$ is the missile mass (kg);
- $I_y = 48.16$ is the pitch moment of inertia (kg·m^2);
- C_{z0} and C_{m0} are aerodynamic coefficients;
- C_{zq}, $C_{z\delta}$, C_{mq}, $C_{m\delta}$ are aerodynamic coefficient derivatives (rad^{-1});

and airspeed matches the missile ground speed (neglecting wind). We begin by assuming $cos(\alpha) \approx 1$ and

$$Z_\alpha(\alpha) \triangleq \frac{Q_{din}S_mC_{za}(\alpha)}{mV_sM} \quad (23)$$

$$Z_q(\alpha) \triangleq 1 + \frac{Q_{din}S_md_mC_{zq}(\alpha)}{2mV_s^2M^2} \quad (24)$$

$$Z_\delta(\alpha) \triangleq \frac{Q_{din}S_mC_{z\delta}(\alpha)}{mV_sM} \quad (25)$$

$$C_{z0}(\alpha) \triangleq C_{za}(\alpha)\cdot\alpha \quad (26)$$

$$M_\alpha(\alpha) \triangleq \frac{Q_{din}S_md_mC_{ma}(\alpha)}{I_y} \quad (27)$$

$$M_q(\alpha) \triangleq \frac{Q_{din}S_md_m^2C_{mq}(\alpha)}{2I_yV_sM} \quad (28)$$

$$M_\delta(\alpha) \triangleq \frac{Q_{din}S_md_mC_{m\delta}(\alpha)}{I_y} \quad (29)$$

$$C_{m0}(\alpha) \triangleq C_{ma}(\alpha)\cdot\alpha. \quad (30)$$

Hence, (20) – (22) are rewritten as a affine parameter-dependent dynamic model

$$\dot{\alpha} = Z_\alpha(\alpha)\cdot\alpha + Z_q(\alpha)\cdot q + Z_\delta(\alpha)\cdot\delta_p \quad (31)$$

$$\dot{q} = M_\alpha(\alpha)\cdot\alpha + M_q(\alpha)\cdot q + M_\delta(\alpha)\cdot\delta_p \quad (32)$$

$$\begin{aligned} a_{mz} &= V_sMZ_\alpha(\alpha)\cdot\alpha + (V_sMZ_q(\alpha) - V_sM)\cdot q \\ &\quad + V_sMZ_\delta(\alpha)\cdot\delta_p. \end{aligned} \quad (33)$$

Disregarding the aerodynamic drag, and establishing a sea level scenario at Mach 3, we have $V_sM = 1020.8$, $Z_q(\alpha) \approx 1$, $Z_\delta(\alpha) \approx 0.2$, $M_q(\alpha) \approx -2.8$, and it is possible to obtain the following relation between $Z_\alpha(\alpha)$ and $M_\alpha(\alpha)$

$$Z_\alpha(\alpha) = -0.01\ M_\alpha(\alpha) - 5.75. \quad (34)$$

Thus, the missile longitudinal polytopic LPV model $G_m(\theta)$ is

$$\begin{aligned} \begin{bmatrix}\dot{\alpha}\\ \dot{q}\end{bmatrix} &= \begin{bmatrix}-0.01M_\alpha(\alpha) - 5.75 & 1\\ M_\alpha(\alpha) & -2.8\end{bmatrix}\begin{bmatrix}\alpha\\ q\end{bmatrix} + \begin{bmatrix}0.2\\ M_\delta(\alpha)\end{bmatrix}\delta_p \\ a_{mz} &= \begin{bmatrix}-10.208M_\alpha(\alpha) - 5869.6 & 0\end{bmatrix}\begin{bmatrix}\alpha\\ q\end{bmatrix} + \begin{bmatrix}204.2\end{bmatrix}\delta_p. \end{aligned} \quad (35)$$

The model has two time-varying parameters $M_\alpha(\alpha(t))$ and $M_\delta(\alpha(t))$, seen in Fig. 2, depending on the single time-varying measured $\alpha(t)$. Hence,

$$\theta(t) \triangleq \begin{bmatrix}M_\delta(\alpha(t)) & M_\alpha(\alpha(t))\end{bmatrix}^T \quad (36)$$

with the following polytope vertices ξ_i

$$\begin{aligned} \xi_1^T &\triangleq \begin{bmatrix}M_\delta^{min} & M_\alpha^{min}\end{bmatrix} = \begin{bmatrix}297.9 & -432.4\end{bmatrix} \\ \xi_2^T &\triangleq \begin{bmatrix}M_\delta^{min} & M_\alpha^{max}\end{bmatrix} = \begin{bmatrix}297.9 & -212.5\end{bmatrix} \\ \xi_3^T &\triangleq \begin{bmatrix}M_\delta^{max} & M_\alpha^{min}\end{bmatrix} = \begin{bmatrix}365.9 & -432.4\end{bmatrix} \\ \xi_4^T &\triangleq \begin{bmatrix}M_\delta^{max} & M_\alpha^{max}\end{bmatrix} = \begin{bmatrix}365.9 & -212.5\end{bmatrix} \end{aligned} \quad (37)$$

and polytopic coordinates $a_i(t)$

$$\begin{aligned} a_1(t) &= \Delta_{M\delta}(t)\,(1 - \Delta_{M\alpha}(t)) \\ a_2(t) &= \Delta_{M\delta}(t)\,(\Delta_{M\alpha}(t)) \\ a_3(t) &= (1 - \Delta_{M\delta}(t))\,(1 - \Delta_{M\alpha}(t)) \\ a_4(t) &= (1 - \Delta_{M\delta}(t))\,\Delta_{M\alpha}(t) \end{aligned} \quad (38)$$

$$\Delta_{M\delta}(t) \triangleq \frac{M_\delta^{max} - M_\delta(\alpha(t))}{M_\delta^{max} - M_\delta^{min}} \quad (39)$$

$$\Delta_{M\alpha}(t) \triangleq \frac{M_\alpha(\alpha(t)) - M_\alpha^{min}}{M_\alpha^{max} - M_\alpha^{min}}. \quad (40)$$

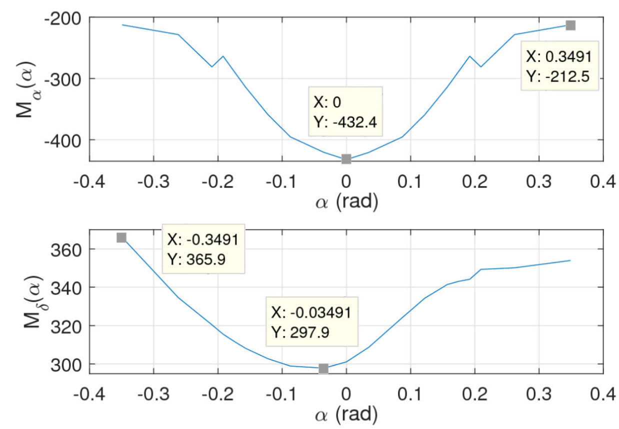

FIGURE 2. **Time-varying parameters $M_\alpha(\alpha(t))$ and $M_\delta(\alpha(t))$ for Mach 3.**

IV. POLYTOPIC H_∞ LOOP SHAPING WITH POLE ASSIGNMENT

This section approaches our proposed methodology. Let's suppose that a polytopic LPV plant is

$$G(\theta) \triangleq \left[\begin{array}{c|c} A_G(\theta) & B_G \\ \hline C_G & 0 \end{array}\right] = \sum_{i=1}^{r} a_i \left[\begin{array}{c|c} A_{Gi} & B_G \\ \hline C_G & 0 \end{array}\right]. \quad (41)$$

Considering the LTI weights W_1 and W_2, only the matrix $A(\theta)$ is parameter-dependent in the shaped plant $G_s(\theta)$, and the traditional H_∞ loop-shaping control solutions are straightforward, such as in [15]. Now, consider our proposed method: weights $W_1(\theta)$ and $W_2(\theta)$ described in a polytopic LPV form, using the same polytopic coordinates of the plant $G(\theta)$

$$W_1(\theta) \triangleq \sum_{i=1}^{r} a_i \left[\begin{array}{c|c} A_{w1i} & B_{w1i} \\ \hline C_{w1i} & D_{w1i} \end{array}\right] \quad (42)$$

$$W_2(\theta) \triangleq \sum_{i=1}^{r} a_i \left[\begin{array}{c|c} A_{w2i} & B_{w2i} \\ \hline C_{w2i} & D_{w2i} \end{array}\right]. \quad (43)$$

Thus, the shaped plant $G_s(\theta) = W_2(\theta)G(\theta)W_1(\theta)$ is

$$G_s(\theta) \triangleq \sum_{i=1}^{r} a_i \left[\begin{array}{c|c} A_i & B_i \\ \hline C_i & 0 \end{array}\right] = \sum_{i=1}^{r} a_i \left[\begin{array}{ccc|c} A_{w1i} & 0 & 0 & B_{w1i} \\ B_G C_{w1i} & A_{Gi} & 0 & B_G D_{w1i} \\ 0 & B_{w2i} C_G & A_{w2i} & 0 \\ \hline 0 & D_{w2i} C_G & C_{w2i} & 0 \end{array}\right]. \quad (44)$$

Differently from previous works (see e.g., [11], [14] [15]), all matrices $A(\theta)$, $B(\theta)$, and $C(\theta)$ are parameter-dependent. By the author's knowledge, we propose an original solution to this theoretical difficulty using the strictly proper definitions of (18) and (41) and employing the Theorem 1, which will be further detailed. Using the four-block generalized plant in (17) and Theorem 1, we obtain the gain-scheduled stabilizing controller $K(\theta)$ in (18). The final controller for $G(\theta)$ is

$$K_F(\theta) = W_1(\theta)K(\theta)W_2(\theta)$$

$$= \sum_{i=1}^{r} a_i \left[\begin{array}{ccc|c} A_{w2i} & 0 & 0 & B_{w2i} \\ B_k C_{w2i} & A_{ki} & 0 & B_k D_{w2i} \\ 0 & B_{w1i} C_k & A_{w1i} & 0 \\ \hline 0 & D_{w1i} C_k & C_{w1i} & 0 \end{array}\right] \quad (45)$$

which evidently is a polytopic LPV system.

Remark 2: In the event the plant model is not in the form of (41), it should be augmented with strictly proper sensors and actuators. The adequate use of filters enables the transfer of the parameter dependence to matrix A, as per the scenario suggested in [20].

Theorem 1: Let's assume that Υ is the LMI region defined in (10). Consider the symmetric matrices $R \in \mathbb{R}^{n\times n}$ and $S \in \mathbb{R}^{n\times n}$, matrices $F,\ L,\ Q_i$ for all $i = 1,\ \ldots,\ r$ of compatible dimensions, and $\gamma > 0$. Consider also the LMI set

$$\begin{bmatrix} S & I \\ I & R \end{bmatrix} > 0 \quad (46)$$

$$\begin{bmatrix} \Psi_i + \Psi_i^T & \bullet & \bullet \\ \left(B_{1i}^T \quad B_{1i}^T R + D_{21}^T L^T\right) & -\gamma I & \bullet \\ \left(C_{1i} S + D_{12} F \quad C_{1i}\right) & D_{11} & -\gamma I \end{bmatrix} < 0 \quad (47)$$

$$2d_1 \begin{bmatrix} S & I \\ I & R \end{bmatrix} + \Psi_i + \Psi_i^T > 0 \quad (48)$$

$$2d_2 \begin{bmatrix} S & I \\ I & R \end{bmatrix} + \Psi_i + \Psi_i^T < 0 \quad (49)$$

defined for all $i = 1,\ \ldots,\ r$, where

$$\Psi_i = \begin{bmatrix} A_i S + B_{2i} F & A_i \\ Q_i & R A_i + L C_{2i} \end{bmatrix} \quad (50)$$

and the convex optimization problem

$$\min_{\gamma,R,S,F,L,Q_i} \{\gamma : 46 - 49\} \quad (51)$$

The full-order, strictly proper dynamic output feedback polytopic LPV controller $K(\theta)$ established by the matrices

$$A_{ki} = (N^T)^{-1}(Q_i - RA_iS - RB_{2i}F - LC_{2i}S)M^{-1} \quad (52)$$

$$B_k = (N^T)^{-1}L \quad (53)$$

$$C_k = FM^{-1} \quad (54)$$

with $N^T M = I - RS$ ensures $J_\infty(T_{zw}(\theta)) < \gamma$ for all $\theta(t) \in \Theta$. Also, the closed-loop poles of $T_{zw}(\theta)$ for all frozen values of $\theta(t) \in \Theta$ remain in Υ.

Proof: We use a known change of variables for this proof (see e.g., [23]). Since Lemma 1 ensures $0 < J_\infty(T_{zw}(\theta)) < \gamma$ for all $\theta(t) \in \Theta$, we start applying the following congruence transformation to (9) with the closed-loop matrices in (19)

$$\begin{bmatrix} T & 0 & 0 \\ 0 & I & 0 \\ 0 & 0 & I \end{bmatrix}^T \begin{bmatrix} A_{cl,i}^T X + X A_{cl,i} & \bullet & \bullet \\ B_{cl,i}^T X & -\gamma I & \bullet \\ C_{cl,i} & D_{cl} & -\gamma I \end{bmatrix} \begin{bmatrix} T & 0 & 0 \\ 0 & I & 0 \\ 0 & 0 & I \end{bmatrix} < 0 \quad (55)$$

$$\begin{bmatrix} T^T(A_{cl,i}^T X + X A_{cl,i})T & \bullet & \bullet \\ B_{cl,i}^T X T & -\gamma I & \bullet \\ C_{cl,i} T & D_{cl} & -\gamma I \end{bmatrix} < 0 \quad (56)$$

defined for all $i = 1, \ldots, r$, where

$$X \triangleq \begin{bmatrix} R & N^T \\ N & V \end{bmatrix} \quad X^{-1} \triangleq \begin{bmatrix} S & M^T \\ M & E \end{bmatrix} \quad T \triangleq \begin{bmatrix} S & I \\ M & 0 \end{bmatrix} \tag{57}$$

and consequently

$$XX^{-1} = \begin{bmatrix} RS + N^T M & RM^T + N^T E \\ NS + VM & NM^T + VE \end{bmatrix} = \begin{bmatrix} I & 0 \\ 0 & I \end{bmatrix} \tag{58}$$

$$X^{-1}X = \begin{bmatrix} SR + M^T N & SN^T + M^T V \\ MR + EN & MN^T + EV \end{bmatrix} = \begin{bmatrix} I & 0 \\ 0 & I \end{bmatrix} \tag{59}$$

$$N^T M = I - RS \tag{60}$$

$$XT = \begin{bmatrix} I & R \\ 0 & N \end{bmatrix} \qquad T^T X = \begin{bmatrix} I & 0 \\ R & N^T \end{bmatrix} \tag{61}$$

$$\begin{aligned} C_{cl,i}T &= \begin{bmatrix} C_{1i} & D_{12}C_k \end{bmatrix} \begin{bmatrix} S & I \\ M & 0 \end{bmatrix} \\ &= \begin{bmatrix} C_{1i}S + D_{12}F & C_{1i} \end{bmatrix} \end{aligned} \tag{62}$$

$$\begin{aligned} B_{cl,i}^T XT &= \begin{bmatrix} B_{1i}^T & D_{21}^T B_k^T \end{bmatrix} \begin{bmatrix} I & R \\ 0 & N \end{bmatrix} \\ &= \begin{bmatrix} B_{1i}^T & B_{1i}^T R + D_{21}^T L^T \end{bmatrix} \end{aligned} \tag{63}$$

$$T^T X A_{cl,i} T = \begin{bmatrix} I & 0 \\ R & N^T \end{bmatrix} \begin{bmatrix} A_i & B_{2i}C_k \\ B_k C_{2i} & A_{ki} \end{bmatrix} \begin{bmatrix} S & I \\ M & 0 \end{bmatrix} = \Psi_i \tag{64}$$

where

$$F \triangleq C_k M \tag{65}$$

$$L \triangleq N^T B_k \tag{66}$$

$$Q_i \triangleq RA_i S + RB_{2i}F + LC_{2i}S + N^T A_{ki} M. \tag{67}$$

Replacing (62) – (64) in (56) yields (47). Now, applying the following congruence transformation in $X > 0$

$$T^T XT > 0 \tag{68}$$

$$T^T XT = \begin{bmatrix} S & M^T \\ I & 0 \end{bmatrix} \begin{bmatrix} R & N^T \\ N & V \end{bmatrix} \begin{bmatrix} S & I \\ M & 0 \end{bmatrix} = \begin{bmatrix} S & I \\ I & R \end{bmatrix} \tag{69}$$

we obtain (46). Again, applying the congruence transformation on both (11) and (12), and recalling the closed-loop polytopic matrices in (19), we have

$$T^T (A_{cl}(\theta)^T X + XA_{cl}(\theta))T + 2d_1(T^T XT) > 0 \tag{70}$$

$$T^T (A_{cl}(\theta)^T X + XA_{cl}(\theta))T + 2d_2(T^T XT) < 0. \tag{71}$$

As a direct consequence of the vertex property [20, theorem 3.3], (70) and (71) hold if and only if they hold at the vertices for the same Lyapunov function X

$$T^T (A_{cl,i}^T X + XA_{cl,i})T + 2d_1(T^T XT) > 0 \tag{72}$$

$$T^T (A_{cl,i}^T X + XA_{cl,i})T + 2d_2(T^T XT) < 0 \tag{73}$$

defined for all $i = 1, \ldots, r$. Using the results from (64) and (69), we obtain (48) and (49). Equations (52) – (54) are obtained from (65) – (67) where we can assume, without loss of generality, that M and N have full row rank [21, lemma 4.2], concluding the proof. □

V. AUTOPILOT DESIGN AND SIMULATION RESULTS

To use the proposed methodology in Section IV, the longitudinal model $G_m(\theta)$ is augmented using both the actuator dynamics $S_1(s)$ and the filter $S_2(s)$, in order to obtain the augmented plant $G_{ag}(\theta) = S_2 G_m(\theta) S_1$. A first-order low-pass filter $S_2(s)$, with a 10^{-3} time constant, is used just for the design. The actuator $S_1(s)$ is a first-order transfer function, with a 0.05 time constant and a 20^o maximum deflection. We also use unitary negative feedback, of pitch rate q, to increase the closed-loop damping, without changing the system polytopic LPV aspect. As a result, the plant $G(\theta)$ to be shaped has the form of (41). We assume ideal inertial sensors, with accelerometers and rate-gyros providing instantaneous, unbiased response. More realistic models of the inertial sensors instead of filter $S_2(s)$ have the disadvantage of increasing the controller order.

The closed-loop system output requirements are as follows:

1) rise time to achieve 100% lower than 0.3;
2) settling time (2% criterion) lower than 1;
3) steady-state error lower than 2%;
4) overshoot lower than 20%; and
5) closed-loop poles, referring to the frozen values of $\theta(t)$ in the vertical strip Υ, such that $-1050 < d < 0$.

The latter requirement is purposed to avoid high frequencies in the controller dynamics and to facilitate actual implementations.

To shape the plant, we choose $W_1(\theta)$ as a first-order low-pass filter $1/(\eta s + 1)$ and $W_2(\theta)$ as a PI filter $(\mu s + \zeta)/s$ with realizations

$$W_1(\theta) = \sum_{i=1}^{4} a_i W_{1,i} \triangleq \sum_{i=1}^{4} a_i \left[\begin{array}{c|c} -\eta_i & 1 \\ \hline \eta_i & 0 \end{array}\right] \tag{74}$$

$$W_2(\theta) = \sum_{i=1}^{4} a_i W_{2,i} \triangleq \sum_{i=1}^{4} a_i \left[\begin{array}{c|c} 0 & \zeta_i \\ \hline 1 & \mu_i \end{array}\right] \tag{75}$$

where η_i, ζ_i, and μ_i are parameters set using the bellow procedure:

1) singular values of the $G_s(\theta)$ are inspected at all vertices, and the weights are adjusted;
2) Theorem 1 is used to find $K(\theta)$; and
3) the behavior of the closed-loop system with $K_F(\theta)$ is assessed at all vertices.

We repeat this process until the requirements are met, and the stability margin achieves an acceptable value. The final tuned values are $\eta_1 = \eta_3 = 150$, $\eta_2 = \eta_4 = 300$, $\mu_1 = \mu_3 = 0.003$, $\mu_2 = \mu_4 = 0.0015$, $\zeta_1 = 0.10$, $\zeta_2 = 0.05$, $\zeta_3 = 0.09$, and $\zeta_4 = 0.045$. Fig. 3 shows the singular values of the shaped (red solid lines) and unshaped (magenta dash-dot lines) plants. Using our proposed method, we obtain very similar red curves, by means of shaping the singular values individually at the vertices. Also, the closed-loop response to an acceleration unitary step input meets the requirements at all vertices, as seen in Figs. 4 and 5. The pole assignment avoids high frequencies in the controller dynamics

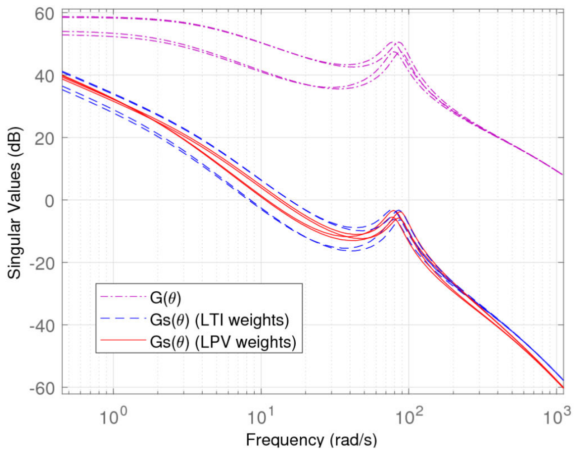

FIGURE 3. Singular values at all four vertices of the unshaped and shaped plants.

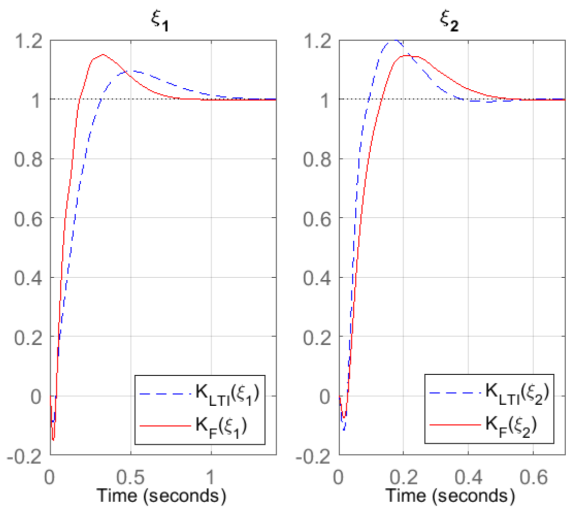

FIGURE 4. Closed-loop response to acceleration unitary step input at vertices 1 and 2.

and the performance achieved is $J_\infty(T_{zw}(\theta)) < 2.74$ for all $\theta(t) \in \Theta$ with the stability margin $\epsilon_0 > 0.364$. The output feedback $K_F(\theta)$ is a four-vertex polytope, eighth-order controller.

We compare $K_F(\theta)$ to a controller named $K_{LTI}(\theta)$, obtained using traditional LTI weights and $A_k(\theta), B_k(\theta), C_k(\theta), D_k(\theta)$. To ensure a fair comparison, we set the parameters using the same procedure for both controllers and tried to satisfy the same requirements regarding the closed-loop system behavior. The weights have the same structure of (74) and (75) but the parameters have to be the same for all vertices (because they are LTI). After several procedure repetitions, the parameters are set as $\eta = 300$, $\mu = 0.002$, and $\zeta = 0.06$. As seen in Figs. 4 and 5, $K_{LTI}(\theta)$ does not achieve the requirements because the rise time is higher than 0.3 at vertex 1, and the maximum overshoot is surpassed at vertex 4. Attempts with faster responses at vertices 1 and 3 surpass the overshoot constraint at vertices 2 and 4, and vice versa.

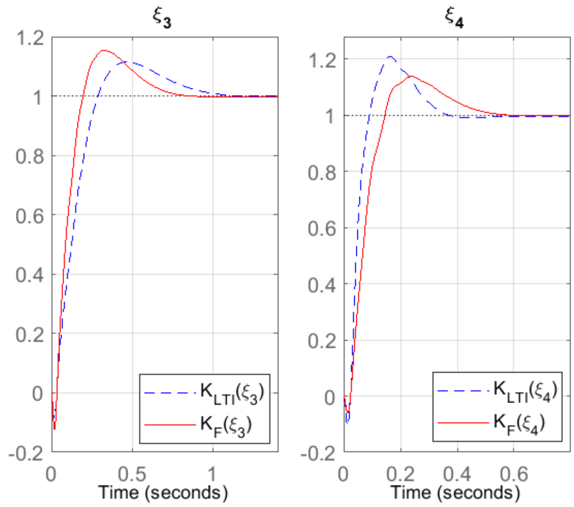

FIGURE 5. Closed-loop response to acceleration unitary step input at vertices 3 and 4.

This is a limitation carried by the traditional method. Shaped plant singular values have different curves at low frequencies, please check the blue dashed lines in Fig. 3. The performance is $J_\infty(T_{zw}(\theta)) < 3.05$ and, consequently, displays an eroded robustness $\epsilon_0 > 0.327$.

Until now, both controllers were designed using the missile polytopic LPV model, and tested only at the vertices of the polytope. To validate the proposal and assess both performance and robustness, we tested the longitudinal autopilot in Simulink using 2-degree-of-freedom nonlinear simulations [see (20) – (22)]. We assumed constant Mach, thus disregarding aerodynamic drag. Such an assumption limits the application to within a specific Mach range. The autopilot is tested in a supersonic flow regime beyond Mach 2. The design presented in the example is not valid in the subsonic and transonic airflow regimes. Angle of attack measurements are assumed available. In practice, α calls for estimation. Wind and α estimation error are disturbances the proposed design approach must accommodate. Autopilot is robust to small disturbances embedded in the normalized coprime factorization of the missile dynamics model uncertainty. $cos(\alpha) \approx 1$ constrains the polytopic LPV model to small α variations (-20^o to $+20^o$ are acceptable).

According to the design, the control was comprised of the controller output and the q feedback. We compared the closed-loop response to the 150 m/s^2 acceleration step input, please refer to Figs. 6 and 7. At $M = 3.8$ (high dynamic pressure), $K_F(\theta)$ obtained a faster response, as expected from the design, with a damping similar to $K_{LTI}(\theta)$. At $M = 2.2$ (low dynamic pressure), $K_F(\theta)$ yielded a faster and better damped response. In both cases, and both controllers, the actuator deflections were realistic and acceptable. The numerical integration with fourth-order Runge-Kutta used a 10^{-3} fixed step. Without the pole assignment, we had to resort to a 10^{-7} fixed step, resulting in a much heavier simulation workload.

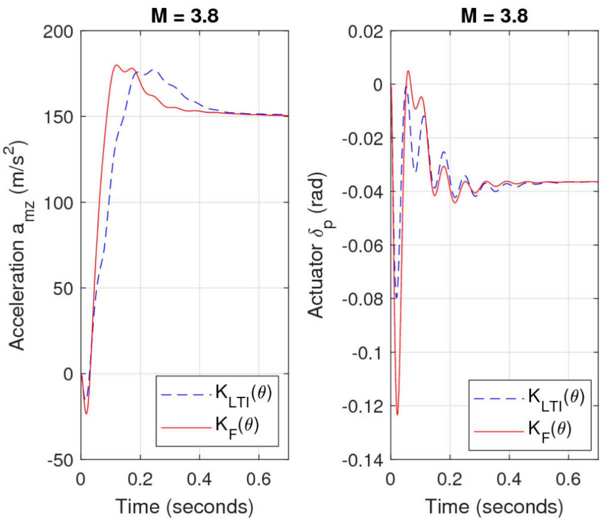

FIGURE 6. Nonlinear closed-loop response and actuator deflection at high dynamic pressure.

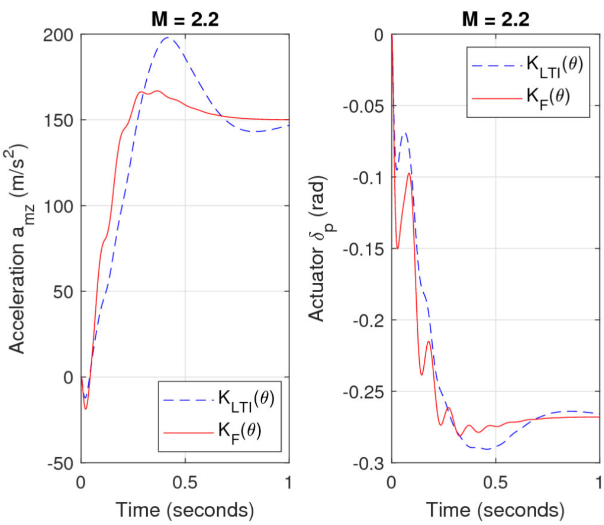

FIGURE 7. Nonlinear closed-loop response and actuator deflection at low dynamic pressure.

VI. CONCLUSION

We propose a novel procedure to obtain an output feedback controller that ensures robust H_∞ performance and stability to a polytopic LPV plant. It is applied to a missile longitudinal model and uses real-time information of the plant to smooth out the gain-scheduling. Our approach is based on polytopic LPV weights, related to the LPV plant concerning of its polytopic coordinates. This can be perceived as a natural extension of the traditional method that uses LTI weights. We also include LMI conditions for assigning closed-loop poles, referring to frozen values of the scheduling variables, hence circumventing controller order reduction such as in [17]. In both high and low dynamic pressure scenarios, nonlinear simulation results show an improved robust stability margin and an improved response to acceleration command, concerning the LTI-weight approach. Future applications are expected to include robust control to flexible aircrafts, long range missiles, and unmanned helicopters. A synthesis limitation of the proposed method is the restriction to use a strictly proper stabilizing controller $K(\theta)$ and a strictly proper shaped plant $G_s(\theta)$. Further research should look into how to circumvent this theoretical issue. We expect to investigate Mach number as a scheduling variable extending the controller operation to interception paths with wide ranges. A disadvantage of the method arises when the number of polytope vertices grow exponentially, with the number of time-varying parameters taken into consideration in the polytopic LPV plant. Manual tuning becomes a daunting task. Machine learning techniques seem suitable and call for further investigation to set the LPV weights automatically. Another challenge is to extend our polytopic H_∞ loop-shaping approach to static LPV controllers.

ACKNOWLEDGMENT

The authors would like to thank the valuable contribution of the missile nonlinear aerodynamics model, designed by Gabriel A. Evangelista from Marinha do Brasil (Brazilian Navy).

REFERENCES

[1] E. Prempain, I. Postlethwaite, and D. Vorley, "A gain scheduled autopilot design for a bank-to-turn missile," in *Proc. Eur. Control Conf. (ECC)*, Porto, Portugal, Sep. 2001, pp. 2052–2057.
[2] D. C. McFarlane and K. Glover, "Robust controller design using normalized coprime factor plant description," in *Lecture Notes in Control and Information Sciences*. Heidelberg, Germany: Springer, 1990.
[3] J. P. Friang, G. Duc, and J. P. Bonnet, "Robust autopilot for a flexible missile: loop-shaping H$_\infty$ design and real ν-analysis," *Int. J. Robust Nonlinear Control*, vol. 8, pp. 129–153, Dec. 1998.
[4] E. Prempain and I. Postlethwaite, "Static H$_\infty$ loop shaping control of a fly-by-wire helicopter," *Automatica*, vol. 41, no. 9, pp. 1517–1528, Sep. 2005.
[5] J. Tang, C. Wei, and F. Yang, "Static H$_\infty$ loop-shaping control for unmanned helicopter," in *Proc. 10th World Congr. Intell. Control Automat.*, Beijing, China, 2012, pp. 2882–2886.
[6] A. Mahmood, Y. Kim, and J. Park, "Robust H$_\infty$ autopilot design for agile missile with time-varying parameters," *IEEE Trans. Aerosp. Electron. Syst.*, vol. 50, no. 4, pp. 3082–3089, Oct. 2014.
[7] J. Li, Z. Yang, Q. Zhang, C. Xu, and H. Xu, "A H$_\infty$ loop shaping control for a quadcopter with tilting rotor," in *Proc. IEEE CSAA Guid., Nav. Control Conf.*, Xiamen, China, Aug. 2018, pp. 1–7.
[8] V. Raghuraman, "Modeling and H-infinity loop shaping control of a vertical takeoff and landing drone," M.S. thesis, Dept. Elect. Electron. Eng., Arizona State Univ., Tempe, AZ, USA, 2018.
[9] Y. Nesterov and A. Nemirovskii, *Interior-Point Polynomial Algorithms in Convex Programming*. Philadelphia, PA, USA: SIAM, 1994.
[10] J. S. Shamma and M. Athans, "Guaranteed properties of gain scheduled control for linear parameter-varying plants," *Automatica*, vol. 27, no. 3, pp. 559–564, May 1991.
[11] E. Prempain and I. Postlethwaite, "Output feedback H$_\infty$ loop-shaping controller synthesis," in *Mathematical Methods for Robust and Nonlinear Control*. Heidelberg, Germany: Springer, 2007, pp. 175–194.
[12] K. Natesan, D. W. Gu, and I. Postlethwaite, "Design of static H$_\infty$ linear parameter varying controllers for unmanned aircraft," *J. Guid., Control, Dyn.*, vol. 30, no. 6, pp. 1822–1827, Nov. 2007.
[13] R. L. Pereira and K. H. Kienitz, "Design and application of gain-scheduling control for a hover: Parametric H$_\infty$ loop shaping approach," in *Proc. 9th Asian Control Conf.*, Istanbul, Turkey, 2013, pp. 1–6.

[14] R. L. Pereira, K. H. Kienitz, and F. H. D. Guaracy, "Discrete-time static H_∞ loop shaping control for LPV systems," in *Proc. 25th Medit. Conf. Control Automat.*, Valletta, Malta, 2017, pp. 619–624.

[15] L. Bergmann, L. Liu, N. Pham, B. Misgeld, S. Leonhardt, and C. Ngo, "Implementation of LPV H_∞ loop-shaping control for a variable stiffness actuator," *IFAC-PapersOnLine*, vol. 53, no. 2, pp. 10129–10134, 2020.

[16] P. Apkarian, P. C. Pellanda, and H. D. Tuan, "Mixed H_2/H_∞ multi-channel linear parameter-varying control in discrete time," *Syst. Control Lett.*, vol. 41, no. 5, pp. 333–346, Dec. 2000.

[17] P. C. Pellanda, P. Apkarian, and H. D. Tuan, "Missile autopilot design via a multi-channel LFT/LPV control method," *Int. J. Robust Nonlinear Control*, vol. 12, no. 1, pp. 1–20, 2002.

[18] V. T. Vu, V. D. Tran, M. H. Truong, O. Sename, and P. Gaspar, "Improving wheelset stability of railway vehicles by using an H_∞/LPV active wheelset system," *Periodica Polytechnica Transp. Eng.*, vol. 49, no. 3, pp. 261–269, Sep. 2021.

[19] İ. H. Şahin and C. Kasnakoğlu, "Control of a small helicopter with linear matrix inequality-based design assuring stability and performance," *Proc. Inst. Mech. Eng., G, J. Aerosp. Eng.*, vol. 234, no. 3, pp. 624–639, Mar. 2020.

[20] P. Apkarian, P. Gahinet, and G. Becker, "Self-scheduled H_∞ control of linear parameter-varying systems: A design example," *Automatica*, vol. 31, no. 9, pp. 1251–1261, Sep. 1995.

[21] M. Chilali and P. Gahinet, "H_∞ design with pole placement constraints: An LMI approach," *IEEE Trans. Autom. Control*, vol. 41, no. 3, pp. 358–367, Mar. 1996.

[22] K. Zhou, J. C. Doyle, and K. Glover, *Robust and Optimal Control*. Englewood Cliffs, NJ, USA: Prentice-Hall, 1996.

[23] C. Scherer, P. Gahinet, and M. Chilali, "Multiobjective output-feedback control via LMI optimization," *IEEE Trans. Autom. Control*, vol. 42, no. 7, pp. 896–911, Jul. 1997.

YURI M. TAVARES was born in Niterói, Rio de Janeiro, Brazil, in November 1985. He received the B.S. and M.S. degrees in electronic engineering from the Universidade do Estado do Rio de Janeiro (Rio de Janeiro State University-UERJ), Brazil, in 2009 and 2016, respectively. He is currently pursuing the Ph.D. degree in systems and control with the Instituto Tecnológico de Aeronáutica (Technology Institute of Aeronautics-ITA), São José dos Campos, São Paulo, Brazil.

Since 2010, he has been with Brazilian Navy. His research interests include guided weapons, image tracking, embedded systems, robust control, and linear matrix inequalities.

JACQUES WALDMANN was born in Brazil, in May 1961. He received the B.Sc. degree in mechanical engineering from the Pontifícia Universidade Católica do Rio de Janeiro (PUC-RJ), Rio de Janeiro, Brazil, in 1983, the M.Sc. degree in aeronautical engineering from the Instituto Tecnológico de Aeronáutica (ITA), Brazil, in 1986, and the D.Sc. degree from the Technion-Israel Institute of Technology, Haifa, Israel, in 1992.

He is a Full Professor with the Department of Systems and Control, ITA. His teaching and research interests include estimation and control in a wide range of aerospace applications, guidance and navigation of autonomous vehicles in GPS-denied conditions, SLAM, computer vision, sensor fusion, and distributed estimation in wireless camera networks for surveillance and threat tracking.